Ocean and Coastal Research

Original Article
Special Article Collection
Carrerette & Bendia (eds), Biology and Geochemistry of seabed pockmark and carbonate mound habitats

http://doi.org/10.1590/2675-2824070.22071fmn
ISSN 2675-2824

Methane-related community of a carbonate-enriched pockmark, Brazilian Southeastern continental slope

Fernanda Mancini Nakamura[1,*], Rafael Andre Lourenço[1], Caio Augusto Magalhães[1], Amanda Gonçalves Bendia[1], Ana Carolina de Araújo Butarelli[1], Julia Gasparini Passos[1], Luiza Ferreira Soares[1], Raissa Basti Ramos[1], Tailisi Hoppe Trevizani[1], Camila Negrão Signori[1], Michel Michaelovitch de Mahiques[1,2], Paulo Yukio Gomes Sumida[1], Vivian Helena Pellizari[1]

[1] Universidade de São Paulo - Instituto Oceanográfico (Praça do Oceanográfico, 191 - Butantã - São Paulo - 05508-120 - SP - Brazil)
[2] Universidade de São Paulo - Instituto de Energia e Ambiente (Av. Prof. Luciano Gualberto, 1289 - Butantã - São Paulo - 05508-900 - SP - Brazil)

* Corresponding author: fe.manak@gmail.com

Abstract

Pockmarks are geological features that often sustain hydrocarbon-related communities of microorganisms when active, seeping oil or methane. Microbial communities of inactive pockmarks have not been well studied until the present. Plenty of pockmarks in the Southwestern Atlantic Ocean have been discovered. However, no information is available about the organic characteristics in association with the microbial diversity related to methane and non-methane hydrocarbon consumption. This study examined the identity and potential ecology of the methane-related microbial community in an inactive SW Atlantic Carbonate-enriched Pockmark (SWACP). Undisturbed sediment cores were enriched with CH_4 99.5% at 5°C, with samples harvested at 16h, 120h, 240h, 720h, and 960h, followed by metataxonomics functional prediction, and the correlation of microbial groups with incubation and enrichment types. The SWACP is depleted in organic compounds, and chemosynthetic production is dominant. Incubated mini-cores of sediment were affected by incubation time and enrichment type, which influenced the microbial composition. Although several taxa were shared among all sediment samples, specific groups per enrichment type and incubation time were observed. These communities comprised taxa previously reported in marine bottom waters, carbonate crusts, active cold-seeps, and inactive pockmarks. The methane-enriched taxa were predominantly related to aerobic methanotrophy, methylotrophy, aerobic and anaerobic non-methane hydrocarbon degradation, and fermentation. This study brings the first survey of the key microbial groups in methane fluxes of a Brazilian deep-sea pockmark, providing data for understanding the ecology surrounding the SW Atlantic gas field areas.

Descriptors: 16S rRNA gene, hydrocarbon, Methanotrophs, Methylotrophs, Fermenters.

INTRODUCTION

Pockmarks are crater-like depressions formed by the collapse of the soft shallow marine seabed from the reduction of subsurface hydrocarbon expulsion pressure related to seepages (Sumida et al., 2004) and are commonly found in oil and gas fields (Haverkamp et al., 2014). These structures are found in different environments, including the continental slope and deep basin seabeds (Sumida et al., 2004). They are present in all oceans, offer a diverse geological history of sediment deposition, and are variable in size and morphology (Marcon et al., 2013), receiving different sedimentation fluxes and temperatures influenced by water masses (Paull et al., 2002). Several pockmarks

Submitted: 09-June-2022
Approved: 26-Oct-2022

Associate Editor: Orlemir Carrerette

in the Southwestern (SW) Atlantic have been described, including in the Santos Basin in the Southeastern - SE Brazilian margin (Figueiredo et al., 1999; Sumida et al., 2004; Schattner et al. 2016; de Mahiques et al., 2017), which consists of a rich deep-water hydrocarbon province (Maly et al., 2019) representing the most productive offshore oil and gas fields of Brazil.

Inactive pockmarks can still leak small amounts of hydrocarbons and even trap gas within the sediment (Haverkamp et al., 2014), making them rich in methane, hydrogen sulfide, sulfate, and ammonium (Conway, 1994). Despite the main thermogenic origin in deep sedimentary systems, hydrocarbons are also synthesized by organisms such as prokaryotes, plankton, and algae in biosynthetic products, which in turn are sedimented through the marine snow and transformed by abiotic processes or consumed by microorganisms as an energy source (Wilkes, Jarling and Schwarzbauer, 2020). In this way, pockmarks can sustain micro- and macroorganisms based on hydrocarbons (Dando et al., 1991; Sibuet and Olu, 1998) and complex carbohydrates that are distinct from the surrounding sediment (Haverkamp et al., 2014). Hydrocarbon, including methane, utilization in pockmarks was addressed in the water-sediment interface of the Baltic Sea (Pimenov et al., 2008), as well as in studies involving water-dissolved methane consumption in active cold seeps (Joye et al., 2004). Asphalt seeps were described on the SE Brazilian margin. However, studies are lacking regarding pockmark microbial ecology and biogeochemical roles in the deep-sea.

The culture-independent approach based on DNA combined with undisturbed sediment enrichment, preserving the stratification of nutrients, cells, and gas, is a powerful technique to identify a target microbial community without modifying the local conditions nor requiring cultivation. The additional 16S rRNA gene amplicon-sequencing in the metataxonomics and the functional prediction allow for the inference of metabolic potentials and attribute effects on the biogeochemical cycles in a given environment (Mann et al., 2010). To characterize a marine inactive carbonate-enriched pockmark in the SW Atlantic through its methane-related community, we enriched undisturbed sediment cores with methane, evaluated its consumption, and identified the taxonomy of the differentially abundant prokaryotes in enriched sediments through 16S rRNA gene DNA amplicon-based next-generation sequencing, and attributed their ecology through functional prediction. The following hypotheses were tested: (a) once the carbonate-enriched pockmark is a hydrocarbon-rich system, the microbiota associated with the methane cycle must be enriched and able to consume the available methane; (b) the by-products from the methanotrophic pathway will favor the enrichment of methylotrophs and heterotrophs; (c) in anoxic layers, the methanotrophic by-products will enrich fermenters and methanogens, leading to a release of methane to the headspace.

This study is the first report of the methane-related microbiota of a pockmark on the Brazilian SE margin gas field region, providing data for understanding the ecology surrounding the current and past active methane seeping areas of the SW Atlantic.

METHODS

Study site

The Southwestern Atlantic Carbonate-enriched Pockmark (SWACP) is located at a depth of 765 m on the Brazilian SE continental slope (-24.5221 and -43.9308). The region is composed of diverse mounds and depressions (Maly et al., 2019) where gas fields are located, and the station is located along the alignment of 35-km long carbonate mounds adjacent to the ACCR complex (May et al., 2019) (Figure 1). The absence of gas flux in acoustic profiling during the expedition confirms the pockmark's relative inactivity.

Sediment sampling

This study is part of the of the multidisciplinary project "Biology and Geochemistry of Oil and Gas Seepages, SW Atlantic (BIOIL)" (IO-USP/ Shell Brasil/ANP), the first expedition for which was in November 2019 aboard the R/V Alpha Crucis of the Oceanographic Institute of the University of São Paulo (IO-USP), described in Sumida et al. (2022). One box corer of 50 x 50 x 50 cm was sampled on the pockmark flank at station ST 681,

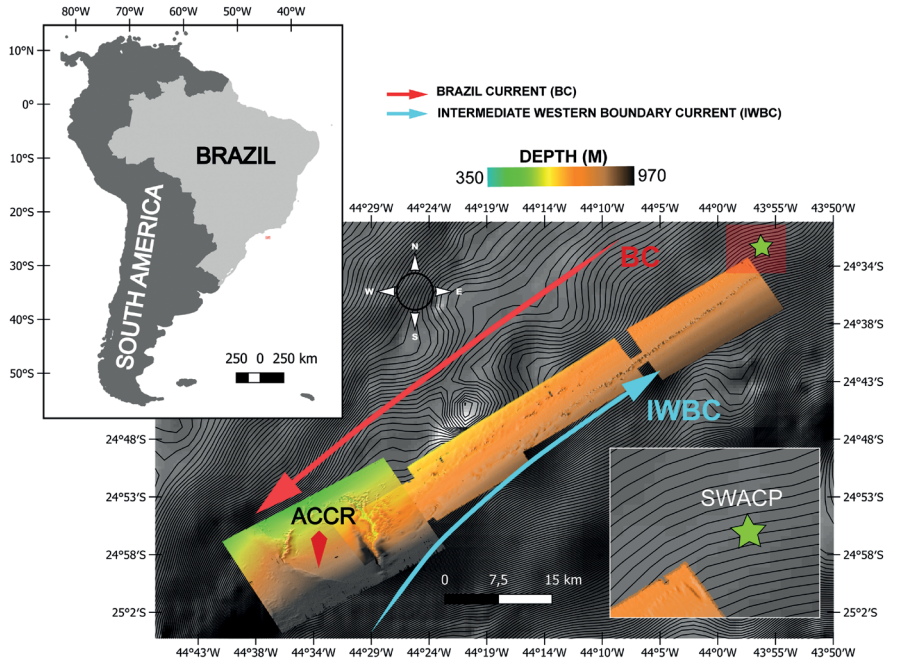

Figure 1. Sampling map in the Santos Basin showing the location of the SW Atlantic carbonate-enriched pockmark (SWACP). The expedition was carried out in November 2019 onboard the R/V Alpha Crucis (IO-USP).

north of the Santos Basin (Area 1). The sediment sample shows a prevalence of calcium carbonate-rich sand and mud ($CaCO_3$ = 22.78%). Deep-sea corals of species *Enallopsammia rostrata*, *Solenosmilia variabili*s, and *Desmophyllum pertusum* are also present in the box-core sample. Metals ratios of the corals indicate nutrient enrichment in the region (Trevizani et al., 2022). The sediment is homogeneous gray until 20 centimeters below the seafloor (Figure SF1).

Seven undisturbed sediment mini-cores (10 x 2 cm) of 50 g wet weight were collected in 60 cc syringes using a manual vacuum-generated 200-cc syringe, preserving the sediment structure. The mini-cores were immediately sealed with bottom rubber caps and upper 3-way syringe taps. The headspace of the intact mini-cores was oxygen depleted with an argon flush, and mini-cores were stored vertically at 4°C for further incubation with methane and molecular analyses onshore. Sediment for dark carbon fixation and heterotrophic microbial production analyses was collected from 3 corers (7 x 20 cm) per box-corer, and extruded and stored in Whirl-pack bags at -80°C. Sediment samples for organic geochemical analyses were collected and stored in aluminum containers and kept frozen at -20°C.

Sediment geochemical analyses and microbial processes determination

A group of seven sterols were selected for analysis in the sediment samples: (1) C_{27} sterols: cholestanol (5α(H)-cholestan-3β-ol—27Δ^0), cholesterol (cholest-5-en-3β-ol—27Δ^5); (2) C_{28} sterols: brassicasterol (24-methylcholest-5,22-dien-3β-ol -28$\Delta^{5,22E}$), campesterol (24-methylcholest-5-en-3β-ol - 28Δ^5); (3) C_{29} sterols: stigmasterol (24-ethylcholest-5,22(E)-dien-3β-ol—29$\Delta^{5,22E}$), β-sitosterol (24-ethylcholest-5-en- 3β-ol - 29Δ^5), and β-sitostanol (24-ethyl-5α-cholestan-3β-ol -29Δ^0). n-Alcohols from n-C_{12} to n-C_{30} were considered. The analyzed hydrocarbons consisted in the 16 EPA-priority PAH further than dibenzothiophene, benzo[e]pyrene, and alkylated homologues (C_1–C_4-naphthalenes, C_1–C_3-fluorenes, C_1–C_3-dibenzothiophenes, C_1–C_4-phenanthrenes–anthracenes, C_1–C_2-fluoranthenes-pyrenes, C_1–C_2-chrysenes), and the aliphatic hydrocarbons (n-alkanes n-C_{12} to n-C_{36}, pristane, phytane). The analytical procedure for the analysis of the organic compounds was reported by Lourenço et al. (2021) and is detailed in the (Supplementary Material SM1).

The calcium carbonate content was determined through gravimetric analysis of the weight difference before and after acidification of each sample using 2M HCl. Total organic carbon, total nitrogen, and $\delta^{13}C$ (reported in ‰ PDB) analyses were performed using a Costec elemental analyzer (EA) coupled to a Thermo Scientific Delta Advantage isotopic ratio mass spectrometer (IRMS) after complete elimination of calcium carbonate from the samples using 2M HCl. $\delta^{15}N$ (reported in ‰ Air) was also analyzed by EA-IRMS using non-decarbonated samples.

The rates of the dark carbon fixation (DCF) and heterotrophic microbial production (HMP) used *in situ*-simulated incubations and were represented in production rates of carbon per area and time ($\mu gC\ m^{-3}\ h^{-1}$). The analytical procedure is detailed in the Supplementary Material SM2.

Methane microcosms' experimental design

We intended to enrich the community with affinity to methane on a simulation of a cold-seep discharge with the injection of a high amount of methane. The seven intact mini-cores, containing 46.65 ± 6.91 g of sediment, 3.87 ± 2.25 mL of tube headspace, and a tube headspace/sediment ratio of 0.90 ± 0.07, were changed by CH_4 99.9% (Whyte Martins, USA) at rates of 200, 000 – 500, 000 ppmv, a mean of 15,478.87 $nmol.L^{-1}$. The intact mini-cores were then randomly disposed of in tube racks inside the incubator BOD TE-371 (Tecnal, Brazil) and incubated at 5°C. The intact mini-cores were distributed into five groups of kill samples, harvested, and destroyed after 16h, 120h, 240h, 720h, and 960h of incubation. After 480h, the samples 720h and 960h had the headspace changed by a new methane injection. Thus, samples from 16h to 240h were 1 time-flushed (1TF), and samples of 720h and 960h of incubation were 2 times-flushed (2TF). Negative controls flushed only with argon were set at the beginning (16h) and end (960h) of incubation. The harvested headspaces were stored in airtight serum vials, closed with sterile butyl-rubber stoppers (autoclaved) and crimp caps, and kept up to the measurement in gas chromatography. Harvested sediment samples were immediately frozen at -20°C for DNA extraction. The 0-10 cm sediment samples were separated in strata of 0-5 cm and 6-10 cm. Only the first stratum was used.

Methane oxidation rate estimation

Headspace methane was quantified in a gas chromatograph (GC6850, Agilent Technologies) equipped with a flame ionization detector (FID) and a 0.1 mL sample loop. A methane standard curve was generated using CH_4 99.5% (White Martins) dilution in room air from 1:1 to 1:10. The conversion of GC area to nM (Nakayama et al., 2011) is represented in Equations 1 and 2, and the methane oxidation rate in nmol g^{-1} h^{-1} (Nagel, 2020) is represented in Equation 3. Each day of measurement, a pure CH_4 was standardized. To avoid overestimation and cross-contamination between samples, the column was cleaned with 1 to 3 syringes filled with 0.2µm filtered room air between measurements. When necessary, saturated CH_4 samples were diluted in 0.2µm filtered argon (Ar).

$$Equation\ 1: Standard\ CH_4[nM] = \frac{injected\ CH_4[1 * 10^{-4} L] * Gas\ purity[0.995]}{Molar\ volume\,(22.4\ L)}$$

$$Equation\ 2: Headspace\ CH_4[nM] = \cdot \frac{Sample\ area * Standard\ CH_4[4,441.96nM]}{Standard\ CH_4\ area}$$

$$Equation\ 3: CH_4\ oxidation\ rate\left[nmol * g^{-1} * h^{-1}\right] = \frac{Initial[nmol] - Final[nmol]}{wet\ weight\ sediment[g] * time[h]}$$

DNA extraction and 16S rRNA gene metataxonomics

DNA extraction from the 0-5 cm sediment samples was performed using the DNEasy PowerMax Soil Kit (Qiagen, Germany) with 5 g, modified by a C1 vortex for 20 min, and incubations were at -20°C instead of 2-8°C, for 10 min. The volume of generated DNA (> 1 mL) was concentrated, and the PEG/NaCl with linear polyacrylamide

precipitation was utilized (Bartram et al., 2009) to avoid loss. The amplicon-based next-generation sequencing of the V4 hypervariable region of the bacterial and archaeal 16S rRNA genes, amplified with the primers 515F-Y and 926R (Parada et al., 2015), was developed at the NGS facility (Piracicaba, SP, Brazil) in a single run on the Illumina Miseq platform in a 250 bp paired-ended system. Sequencing data were deposited in the National Center for Biotechnology Information Sequence Read Archives (SRA) under BioProject ID PRJNA840942.

Bioinformatics

Analyses were developed as detailed in Bendia et al. (2021). Raw sequences were imported to QIIME2 (v.2020.2, https://docs.qiime2.org/) (Bolyen et al., 2019) using the q2-tools-import script. After visual inspection of quality profiles, the reads were quality filtered > 28, the forward reads were truncated at position 259, and the reverse reads at 190, using the q2-dada2-denoise script. Primer sequences were removed using the same script. DADA2 denoising was used to obtain a set of Amplicon Sequence Variants (ASV) (Callahan et al., 2017). Alpha and beta diversity metrics were computed through the q2-diversity core-metrics script at a rarefied sampling depth of 30,081 sequences (Figure SF2). Taxonomy was assigned through *feature-classifier classify-sklearn* and SILVA database v.138 trained for the primers 515F-Y and 926R. The phylogenetic tree was built by FastTree (Price et al., 2009) and the MAFFT aligner (Katoh et al., 2009).

Functional Prediction

The assignment to potential functions was performed using the FAPROTAX tool (Louca et al., 2016). The functional prediction used bacterial and archaeal taxonomy as entries for an edited database (this study), developed by the FAPROTAX_1.2.4 database (Louca et al., 2021) amendment with the addition of 2,051 taxonomical entries, 22 new ecological roles based on cultured from IJSEM database (Barberan, 2016) and LPSN database (Parte, 2018), also from direct searches for functions and genes on NCBI (https://www.ncbi.nlm.nih.gov/search/), SILVA database (Yilmaz et al., 2014), and genome and metagenome-assembled genome reports. In addition, commonly found taxa and microbial bioindicators of five habitats were added for ecological characterization. Functions were also revised to allocate those which are interconnected (taxa associated with multiple functions and levels of functions). Our edited database is available at https://doi.org/10.5281/zenodo.7226298. Database amendment details can be found in Supplementary Materials SM3.

Statistics

The richness, Shannon, and InvSimpson diversity indexes were calculated using *phyloseq* (McMurdie and Holmes, 2013) and *vegan* (Oksanen et al., 2013) packages. To compare the structure of the communities among enrichment type and incubation times, a principal coordinate analysis (PCoA) ordination was performed based on Weighted Unifrac distance (Lozupone et al., 2011). To predict the differential abundance of taxa in methane-enriched samples, we compared the controls to the enriched samples (samples at 16h and 960h) in the compositional constraints with *ANCOM* (Mandal et al., 2015), and the significant clr ($W > 4$) were reported using the *ggplot2* package (Wickham et al., 2016). The presence and absence of unique and shared taxa were reported in the UpSet plot using the *UpSetR* package (Conway et al., 2017). The corresponding predicted functions and phylum, or class, were reported with the *ggplot2* package, as well. Spearman's monotonic correlations between the phyla and the enrichment attributes (methane presence or absence, and incubation times) were estimated using the *hmisc* package (Harrell et al., 2019) by applying the $p < 0.05$. To be able to find the phyla that correlate to the methane rates and to a certain enrichment type and incubation time, we developed the approach of disentangling the variable "sample" (with or without methane by their different incubation times) to create the matrix against the ASVs, which were pooled in the taxonomic level phylum. The correlation network was performed using *Gephi* software (Bastian et al., 2009).

RESULTS

Geochemical analysis and microbial production in the SWACP pockmark

The 5 cmbsf sediments showed low rates of dark carbon fixation (DCF) and heterotrophic microbial production (HMP). Considered with the rates of total organic carbon (TOC), isotopic signal $\delta^{13}C$ (reported in ‰ PDB), total nitrogen (TN), and C/N ratio (Table 1), this corresponds to an oligotrophic system. The dissociation between DCF and HMP indicates a predominance of chemoautotrophic processes in the SWACP chemosynthetic system. Although C and N concentrations were deemed at the detection limit, their ratios were used for organic matter qualification.

Biogenic origin of alkanes was evident in the higher rate of long-chain AH (C_{20}-C_{40}) (Table 2). On the other hand, the C_{31}/C_{19} ratio > 0.4 and C_{29}/C_{31} < 1 confirm a terrigenous influence. Although the HMW/LMW-AHs > 1 suggests a petrogenic input, the relative concentration of all AH typical of petroleum was not present. No Pristane was detected, in addition to not being able to calculate TAR and CPI correctly. In addition to the aliphatic hydrocarbons, the amount of methane detected in the sample control-16h indicates *in-situ* methane presence, entrapped in the sediment cores (Table 2).

Target petroleum PAHs, such as Naphthalene, Phenanthrene, Pyrene, Fluorene, Fluoranthene, low rates of Acenaphthylene, Benzo[b]fluoranthene, 2- and 1-Methyl-naphthalene, and Chrysene were at the detection limit (Table 2). Petroleum origin was also evident in the LMH-PAHs dominancy over HMW-PAHs and by the Fluoranthene/Pyrene ratio (0.3). Fluoranthene and Pyrene also suggest pyrolytic origin.

Sterols concentrations (Table 2) were low. Land- and marine-derived organic matter was evident from the occurrence of fatty alcohols C_{16} and C_{28} (Table 2).

Methane consumption in the incubated samples

We observed constant methane consumption with incubation time by the decrease of methane in the headspace (Figure 2a) of 10.18 nmol g^{-1} h^{-1} until 16h (equivalent to 51% of total consumption), 1.83 nmol g^{-1} h^{-1} until 120h (equivalent to 65% of total consumption), 1.10 nmol g^{-1} h^{-1} until 240h (equivalent to 81% of total consumption), 0.51 nmol g^{-1} h^{-1} until 720h (equivalent to 93% of total consumption), and finally 0.34 nmol g^{-1} h^{-1} until 960h (total consumption of methane). The initial environmental methane of 124.11 nM was completely oxidized by the end of the incubation time in the control sample (control-960h).

Alpha and Beta Diversity of the incubated samples

Valid sequences totaled 366,325 (mean 52,332 ± 2,113) among the seven sediment samples, clustered into a mean of 749 amplicon sequence variants (ASVs) (SD ± 40). Methane input and incubation time overall affected the microbial community composition (Figure 2c). Though the lack of change in richness (Shannon) throughout the incubation is indicative of stability in diversity and perhaps functionality of the community, community selection occurred through the decrease of alpha diversity indices of ASVs number, the dominance of groups (InvSimpson), and presence of rare groups (Fisher) (Figure 2b). Looking closely at incubation types (Table ST1), we observed that the initial control sample (control-16h) harbored the vast diversity typical of an environmental sample, which was depleted after 40 days of incubation (control-960h). With respect to methane input, methane oxidation during the first 120h (enriched-120h) exerted selection pressure,

Table 1. Geochemical and microbial data of the SWACP region: carbonate, carbon fractionation, carbon, and nitrogen availability, and microbial production rates of Dark Carbon Fixation and Heterotrophic Microbial Production.

DCF	HMP	TOC	$\delta^{13}C$	TN	C/N	$CaCO_3$
µgC.m^{-3}.h^{-1}	**µgC.m^{-3}.h^{-1}**	%	‰	%	%	%
12513.17	41.33	0.90	-20.86	0.14	6.43	22.78

Table 2. Organic geochemical data of the SWACP region: carbonate, carbon fractionation, carbon, and nitrogen availability, and microbial production rates.

Total per deffinition	***PAH*** µg.kg^{-1} 11.09	***Methane*** nmol.L^{-1} 124.11	***Aliphatic hydrocarbons (AH)*** µg.kg^{-1} 8.67				***Sterols*** µg.kg^{-1} 0.08		***Alcohol*** µg.kg^{-1} 0.06	
			LMW-Ahs 0.97		HMW-AHs 7.64					
Total per molecule type within the deffinition	Naphthalene	5.32		0.28	C22	1.00	β-sitosterol	0.07	C28	0.04
	Phenanthrene	1.55	C15	0.16	C31	0.80	stigmasterol	0.01	C16	0.02
	Pyrene	1.50	C16	0.16	C29	0.61				
	Fluorene	1.19	C19	0.12	C24	0.50				
	Fluoranthene, Acenaphthylene, Chrysene, Benzo[b]fluoranthene, 2- and 1-Methyl-naphthalene	<1	C17, C13, C10, C18	<0.1	C33, C27	0.47				
					C32	0.44				
					C25	0.40				
					C39	0.37				
					C30	0.37				
					C20	0.34				
					C35	0.32				
					C28	0.32				
					C36	0.31				
					C34	0.29				
					C37	0.25				
					C26	0.23				
					C21	0.12				
					C38, Ph	< 0.1				
	LMH-PAHs	9.20			C31/C19 ratio		6.85			
	HMH-PAHs	1.89			C29/C31 ratio		0.77			
	Fluo/Py ratio	0.30			HMW-AHs/LMH-AHs		7.84			
	Fluo/(Fluo+Py)	0.23			Pr/Ph; TAR; CPI		-			

Abbreviations: PAH, Polycyclic Aromatic Hydrocarbons; LMH-PAHs, low-molecular-weight PAHs of 2-3 rings; HMW-PAHs, high-molecular-weight PAHs of 4-5 rings; HMW-AHs, high-molecular-weight AH; LMW-AHs, low-molecular-weight AH; Fluo, Fluoranthene; Py, Pyrene; CPI, Carbon Preference Index; Pr/Ph, pristane and phytane ratio.

lowering the diversity indices of ASVs number (Observed) and richness (Shannon), but increasing evenness (E=Shannon/Observed), leading to community homogenization with lower group dominance (InvSimpson) and lower presence of rare groups (Fisher). The diversity indexes of ASVs number, richness, and rare groups then progressively increased between 240h and 960h (enriched-240h < 720h < 960h), while dominant groups (InvSimpson) only increased toward the end of incubation, between 720h and 960h (enriched-720h < 960h), resulting in a new community with higher diversity indices of ASVs number and richness, with dominant groups, and a higher portion of rare groups (Observed, Shannon, InvSimpson, and Fisher, respectively).

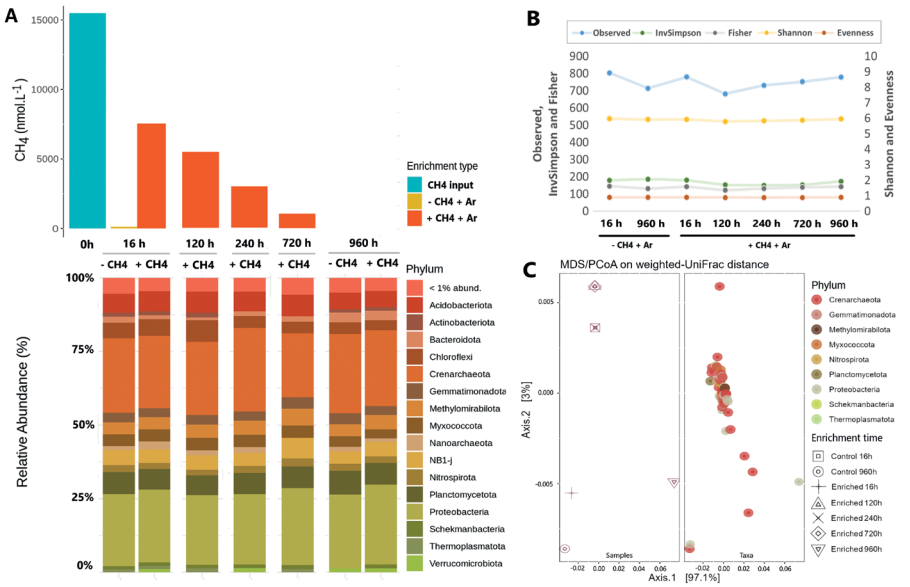

Figure 2. Microbial community composition of deep-sea sediments of a pockmark in the Southwestern Atlantic margin enriched with methane. (A) Methane quantification and respective microbial composition per incubation time and enrichment type; -CH_4 + Ar, Argon incubation in the controls destructive samples harvested at 16h and 960h; +CH_4 + Ar, Argon, and methane incubation in the enriched destructive samples harvested at 16h, 120h, 240h, 720h, and 960h. Sequences were taxonomically classified using the Silva database v. 138. (B) ASVs alpha diversity indexes are grouped by enrichment type. (C) Biplot of PCoA is based on weighted Unifrac distance of the most abundant taxa (>1%) in all samples per enrichment time.

Microbial community composition among incubated samples

Regarding microbial composition per enrichment type, the most abundant phyla in the controls and in the methane-enriched samples were, respectively: Crenarchaeota (25.9 % and 24.9 %), Proteobacteria (24.7% and 25.0 %), Planctomycetota (7.7 % and 7.1 %), Acidobacteriota (6.1% and 6.7 %), NB1-j (4.7 % and 5.1 %), Chloroflexi (4.6 % and 4.8 %), Methylomirabilota (4.1 %, and 4.8 %), Myxococcota (3.8 %, and 3.9 %), Gemmatimonadota (3.4 % and 3.2 %), Nitrospirota (2.3 % and 2.3 %), Bacteroidota (2.7 % and 1.8 %), Nanoarchaeota (1.5 % and 1.7 %), Schekmanbacteria (1.0% and 1.2 %), Actinobacteriota (1.2 % and 1.1 %), Verrucomicrobiota (1.0 % and 1.1 %) (Figure 2a). The community structure at class level is detailed in Figure SF3.

Correlation of the microbial community

Co-occurrence was observed through significant ($p<0.05$) Spearman correlation, suggesting interactions of microbial communities with methane detection and consumption, incubation times, and enrichment types (Figure 3). Overall, methane detection was positively correlated with Acidobacteriota (0.82), Chloroflexi (0.79), and the low-abundant Elusimicrobiota (0.82), while methane detection and oxidation were negatively correlated with Bacteroidota (-0.93, and -0.86, respectively). The control-16h, enriched-16h, and enriched-120h samples showed similar microbial groups, while enriched-720h exhibited diverse correlations. Even more distinct were the control- and enriched-960h samples. Correlations with incubation time were positive between control-16h and the low-abundance TA06 (1.00), besides with the keystone Euryarchaeota (0.76). Euryarchaeota in turn was positively correlated with the low-abundance phyla AncK6 (0.76), Desulfobacterota (0.76), Fibrobacterota (0.94), Hydrogenedentes (0.82), and Marinimicrobia SAR406 clade (0.80). Also, correlations with incubation time were positive between control-960h and Aenigmarchaeota (1.00). Correlations with incubation time in enriched samples were positive between enriched-16h and Asgardarchaeota (1.00),

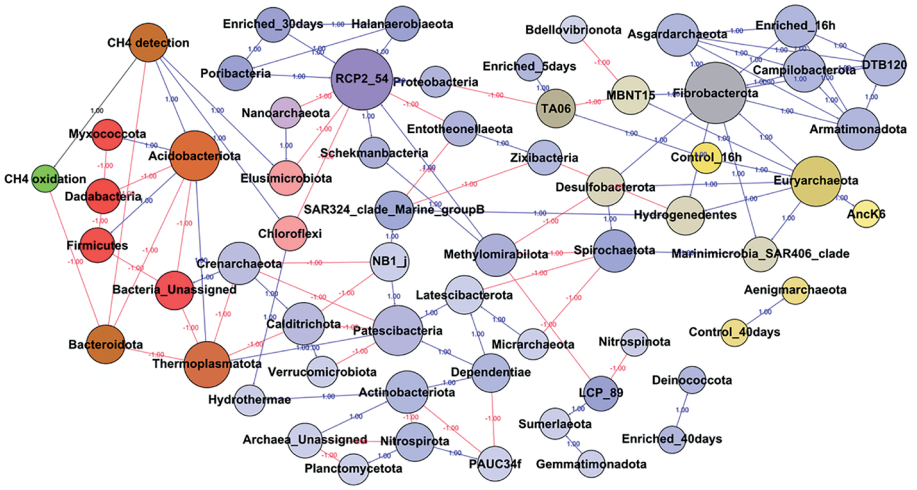

Figure 3. Network analysis based on Spearman rank correlation exhibiting potential interactions of microbial communities with enrichment time and methane detection and consumption in deep-sea pockmark sediments of the Southwestern Atlantic margin. Only significant ($p < 0.05$) Spearman correlations are shown: blue lines, positive correlation; red lines, negative correlation; correlation numbers are indicated in the lines. The circle colors differentiate the variables: green, CH_4 oxidation rate in $nmol.g^{-1}$; red, CH_4 detection in the headspace in nM; yellow, controls; blue, enriched samples; different colors were generated by the superposition of colors. Spearman correlation was performed using *hmisc* in R software. The network was built in *Gephi* 0.9.2.

Armatimonadota (1.00), Campilobacterota (1.00), DTB120 (1.00), Armatimonadota (1.00), and the keystone Fibrobacterota (0.76); positive between enriched-120h and TA06 (0.76), which in turn was negatively correlated with MBNT15 (-0.76) and Proteobacteria (-0.76); positive between enriched-720h and Halanaerobiaeota (1.00), Poribacteria (1.00), and the keystone RCP2-54 (0.76); and finally positive correlation occurred between enriched-960h and Deinococcota (1.00) (Figure 3). The enriched-240h did not show any correlation.

Differentially abundant communities among incubated samples

Differentially-abundant taxa across incubation times and enrichment types are detailed in Figure 4, and the ASVs analysis is detailed in Figure SF4**.** The most significant number of unique taxonomies was found in the methane enriched-16h (47 unique taxa), followed by the control-16h (39 unique taxa). The number then decreased from enriched-16h to enriched-120h (17 unique taxa) and increased again for the enriched-240h (23 unique taxa). For the enriched-720h (the second-time CH_4 flush (2TF)), we detected an increase (38 unique taxa), which persisted through the enriched-960h (37 unique taxa). The control-960h had a lower number of unique taxa (30 unique taxa). Ten shared taxa are related to the 2TF (enriched-30th and enriched-40th days), eight shared taxa are related to 960h incubations (control and enriched), and four taxa remained exclusive to the controls. The ANCOM differential abundance across enrichment types, a pool of control or enriched samples at 16h and 960h, is represented in Figure SF5**.** The differentially-abundant taxa in controls were mainly uncultured.

Functional prediction based on the taxonomy of the incubated samples

Functional prediction was performed over the entire dataset (681 unique taxa from ASVs), and differentially abundant groups were assigned to 50 functions, through which 160 ASVs (23.50%) were assigned to at least one function. In comparison, 521 unique taxa from ASVs (76.50%) had no reference for functional assignment and correspond to uncultured or uncategorized. The functional prediction over the enrichment types (control and enriched), incubation times per enrichment type (controls at 16h and 960h, enriched from 16h to 960h), and the functional prediction over unique,

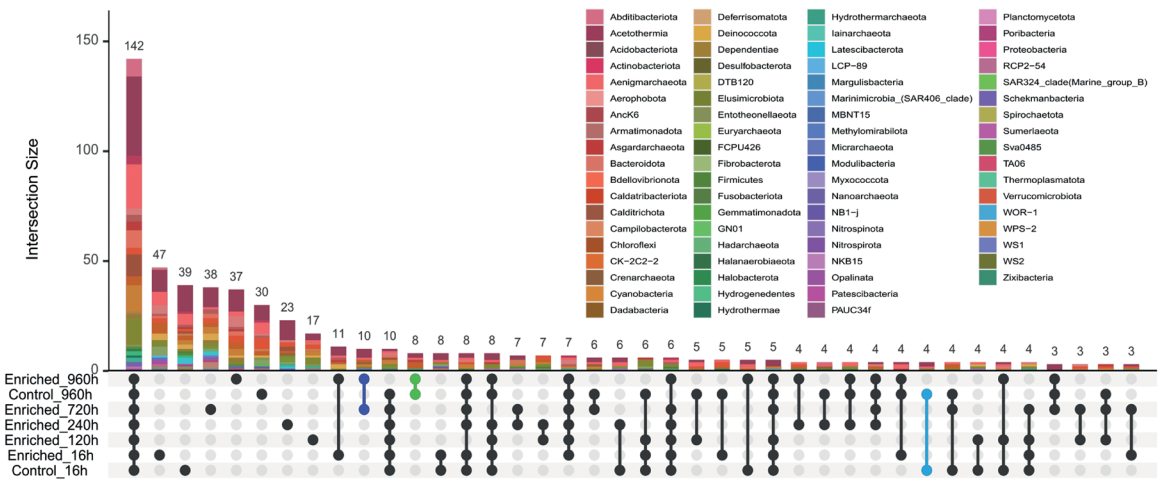

Figure 4. Upset Plot composed of bacterial and archaeal taxonomies identified among ASVs detected on the harvesting times of the methane incubation of deep-sea intact pockmark sediment cores of Southwestern Atlantic margin. Black lines connecting circles indicate shared taxonomies. Black points solely indicate unique taxonomy presence per set. Vertical bars indicate intersection size (number of complete taxonomies, up to Species from the assignment with Silva v.138) on each set. Bar colors represent the taxonomy at the phylum level. Connections colors are described along with the text. Ten shared taxa are related to the 2TF (enriched-30th and enriched-40th days) (purple connection); 8 shared taxa are related to 960h incubations (control and enriched, green connection); 4 taxa remained exclusive of control-16h and control-960h (blue connection).

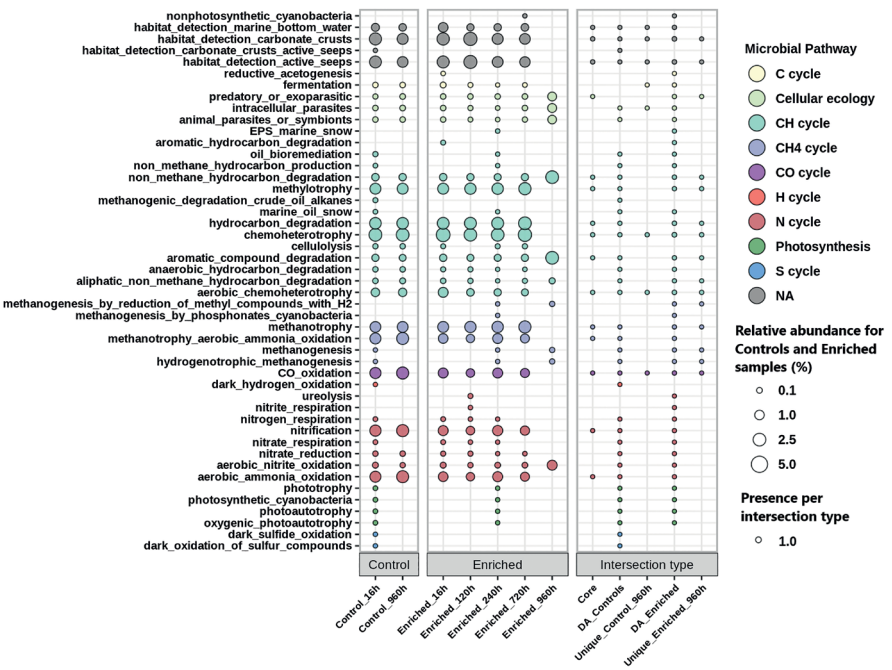

Figure 5. Functional prediction of the microbial community among enrichment types, incubation times, and the differentially abundant methane microcosms of deep-sea pockmark sediment cores of the Southwestern Atlantic margin. Predicted functions and commonly found habitats, y-axis, per intersection type, x-axis; colors indicate the respective microbial pathway. Datasets: taxa are grouped by incubation time and the enriched type and per intersection type, x-axis, in the unique presence of taxa in "Un. Control-960h" and "Un.Enriched-960h"; shared taxa in the entire dataset are represented in "Core"; ANCOM differential abundant taxa (W > 4) between controls and enriched samples (pool of 16h and 960h of each enrichment type) are represented by "Unique_DA_Controls" and "Unique_DA_Enriched". Sequences were taxonomically classified using the Silva database v. 138, and taxonomy-based functionally predicted with the FAPROTAX tool based on an amended database developed in this study.

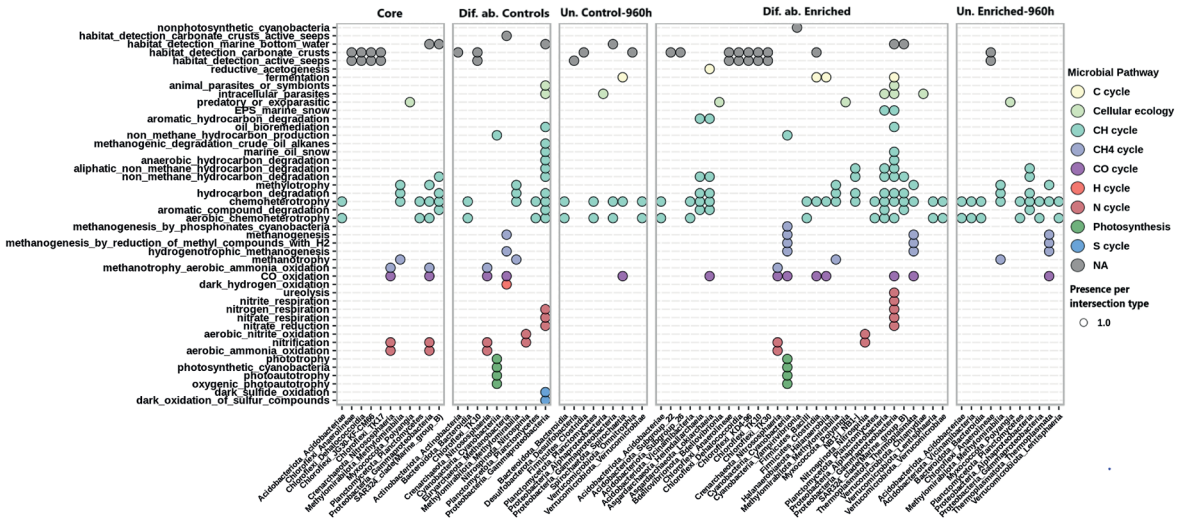

Figure 6. The functional prediction of the microbial community is differentially abundant on the methane microcosms of deep-sea intact pockmark sediment cores of Brazilian SE Atlantic. Predicted functions and commonly found habitats, y-axis, and respective taxa per intersection type at the class level, x-axis; colors indicate the respective microbial pathway. Datasets: taxa are grouped per intersection type, x-axis, in the unique presence of taxa in "Un.Control-960h" and "Un.Enriched-960h"; shared taxa in the entire dataset are represented in "Core"; ANCOM differential abundant taxa (W > 4) between controls and enriched samples (pool of 16h and/to 40th day of each enrichment type) are represented by "Dif. ab. Controls" and "Dif. ab. Enriched". Sequences were taxonomically classified using the Silva database v. 138, and taxonomy-based functionally predicted with the FAPROTAX tool based on an amended database.

shared, and differentially abundant taxa, are represented in Figure 5. The functional prediction per taxonomical record is detailed in Figure 6. The core functions in different levels were aerobic ammonia oxidation and possible methane oxidation, nitrification, carbon oxide oxidation, methylotrophy, aromatic hydrocarbon degradation, and predatory or ectoparasitic taxa (Figure 5), overall with the presence of the phylum Acidobacteria, Chloroflexi, Methylomirabilota, Myxococcota, Plantomycetota, Proteobacteria, and SAR324 Marine Group B (MGB) (Figure 6). The function of dark hydrogen oxidation and detection in carbonate crusts of active seeps, assigned to Euryarchaeota, were only present in the initial sample (control-16h), degrading over the incubation time and with the methane input (Figures 5 and 6). The functions present in the control-960h where chemoheterotrophy represented by Bacteroidota, Planctomycetota, Proteobacteria, Spirochaetota, and Verrucomicrobia, also the fermentation represented by Spirochaetota, and the intracellular parasitism represented by Proteobacteria (Figures 4 and 5). Other than lignin, chitin, xylan, cellulose, methanol, methane, and aromatic hydrocarbons, chemoheterotrophy and specific aerobic chemoheterotrophy are present in both the control-960h and enriched-960h. However, enriched-960h had additional chemoheterotrophic Acidobacterota, Bacteroidota, Planctomycetota, and the common deep-sea Chloroflexi. Other specific groups of enriched-960h, compared to control-960h, would be involved in non-methane aliphatic hydrocarbon degradation (Proteobacteria phylum), methylotrophy (Methylomirabilota and Thermoplasmatota phyla), methanotrophy (Methylomirabilota phylum), and in methanogenesis by reduction of methyl-compounds and hydrogenotrophy (Thermoplasmatota phylum). The enriched-960h lost the Desulfobacterota and Firmicutes phyla associated with active seeps and carbonate crusts, respectively, also losing the chemosynthetic Spirochaetota (Figure 6).

The taxa of the highly methane-enriched sediment (enriched-960h) (Figure 6) were the uncultured Methanomassiliicoccales (Thermoplasmatota), Methylomirabilia, uncultured Rhodobacteraceae, unassigned Colwelliaceae, uncultured Chloroflexi, Acidobacteriae uncultured Subgroup-12, Vicinibacteria uncultured Subgroup-17, Bacteroidia, Planctomycetes, Lentisphaera, and Polyangia. Methanomassiliicoccales is potentially

methylotroph, hydrogenotrophic methanogen, and methanogen by reduction of methyl-compounds using H_2. The Methylomirabilia class is potentially a hydrocarbon degrader, methylotroph, and nitrite-dependent denitrifying anaerobic methane-oxidizing bacteria. The alphaproteobacterial uncultured Rhodobacteraceae is potentially a chemoheterotroph for aromatic and non-methane aliphatic hydrocarbons degradation. The unassigned gammaproteobacterial Colwelliaceae is potentially an aerobic chemoheterotroph by aliphatic non-methane degradation, also a nitrate reducer, as well as involved in fermentation. The uncultured Chloroflexi is commonly found in carbonate crusts and active seeps, not as a biomarker. The actinobacterial Acidobacteriae uncultured Subgroup-12, Vicinibacteria uncultured Subgroup-17, bacteriotal Bacteroidia, Planctomycetes, and the verrucomicrobial Lentisphaera were all assigned as potentially involved in unknown aerobic chemoheterotrophy. The myxococcotal Polyangia was assigned as a potential predator or ectoparasite.

DISCUSSION

Hitherto, the microbial ecology of the Brazilian continental slope pockmarks was unknown, and it was unclear if even inactive pockmarks could represent a hotspot for microbial communities involved in the mineralization of methane. This study first observed methane-related chemosynthetic and heterotrophic microbial communities in carbonate-enriched pockmark sediment over a deep-water hydrocarbon-rich system in the southwestern Atlantic margin. We developed methane enrichments to detect changes in the abundance of community groups in undisturbed sediment cores of a deep-sea pockmark of the Santos Basin, SW Atlantic Ocean. We detected different methane consumption rates and variations in microbial diversity during incubation, attributed to the variation in community structure due to the high selection pressure of the experiment variables. In addition, we identified the taxonomy and potential ecological functions of the bacteria and archaea that were enriched in the presence of the methane provided. Differently than active cold-seeps, which support anaerobic methane-oxidation (AOM) played by ANMEs with developing syntrophy with sulfate-reducers, the dominant microbial groups in these systems (Michaelis et al., 2002), the SWACP sediment harbors a diversity associated with methanotrophy, methylotrophy, and aerobic and anaerobic non-methane hydrocarbons degradation, also involving fermentation and methanogenesis.

Geochemistry of the inactive pockmark sediment

The bulk sediment of the SWACP is composed of high rates of calcium carbonate (Basti et al., 2022) and low amounts of organic compounds. As such, they have similar TOC to other pockmarks (Haverkamp et al., 2014) and to a seep area in the Black Sea Batumi (Blumenberg et al. 2018). The ratios C/N, δ^{13}C/TOC, δ^{13}C/TN, and DCF indicate very depleted organic matter that is typically old and degraded. The TOC/TN (6.43) indicates that marine primary production is the main source of organic matter in the SWACP, originated by chemosynthetic processes as represented by the higher DCF/HMP ratio. The presence of methanotrophy and hydrocarbon degradation in the SWACP could explain the low detection of organic compounds. Local corals represent an additional source of nutrients for the SWACP sediment (Trevizani et al., 2022). However, the nutrients in inactive pockmarks tend to be less abundant than in surrounding sediments, as reported by Haverkamp et al. (2014), in which TOC and TC concentrations differ from reference sediments. The nutrients also tend to be stratified, as the reported TN formed by ammonium and nitrate, and decrease with depth due to nitrate reduction coupled with organic matter degradation (Haverkamp et al. 2014).

The marine hydrocarbon compounds originate from asphalt and cold seeps, as well as significantly from the pelagic system by cyanobacteria (McGenity et al., 2021) sedimented as marine snow. The terrestrial organic matter is an additional source of hydrocarbons for the marine ecosystem (Pusceddu et al., 2009). Despite the very low amounts, when analyzing diagnostic indices, biogenic and terrigenous sources of aliphatic hydrocarbons (AH) were supported by the significant portion of high molecular weight alkanes (HMW-AHs) (Yusoff et al., 2012) and by the C_{31}/C_{19} and

C_{29}/C_{31} ratios, respectively. In addition, pyrolytic and petroleum combustion is the origin of the SWACP polycyclic aromatic hydrocarbons (PAH), indicated by the Fluoranthene and Pyrene rates (Zeng et al., 1997; Wang et al., 1999) and Fluoranthene/(Fluoranthene+Pyrene) ratio (Yunker et al., 2002; Mille et al., 2007; Zrafi et al., 2013).

Aliphatic hydrocarbons (n-alkanes, AH), both linear and cyclic, and polycyclic aromatic hydrocarbons (PAH) are abundant constituents of petroleum (Comandini et al., 2013). The presence of n-alkanes is proportional to the oil integrity, since highly biodegraded oil reserves show low rates of n-alkanes (Wilkes et al., 2020). Despite the low detection of hydrocarbons, the presence of petrogenic sources of hydrocarbons was supported by the HMW/LMW-AHs, the Fluoranthene/Pyrene ratio, and the dominance of LMH-PAHs (Wang et al., 2003). In addition, the presence of target PAHs indicators of petroleum suggests petrogenic sources of hydrocarbons (Wang et al., 2003; Zrafi et al., 2013) and persistence in the SWACP, even at very low concentrations. Furthermore, the occurrence of long-chain alcohols C_{16} and C_{28} suggest land and marine origins (Mudge, 2005), with possible atmospheric transportation from land and sedimentation in the deep-sea bottom, as reported in the deep-sea of the North Pacific (Kawamura, 1995). We conclude that the hydrocarbon and fatty acid dynamics in the SWACP comprise the lateral transference from land to the marine system, exhibiting a local biogenic origin and the presence of petrogenic compounds at low levels.

The marine by-products of hydrocarbon metabolization include the sterols, whose total concentration was low compared to other marine sediments such as coastal South-Central Chile (Saavedra et al., 2014). Sitosterol and stigmasterol concentrations were inferior to compared to the East China Sea Shelf (Jeng and Huh, 2004). Interestingly, stigmasterol and its precursor β-sitosterol are both constituents of sphingosine from marine sponge *Myxilla* sp carbon skeleton (Bunyola et al., 2017), and of marine fish muscle (Ozogul et al., 2015), crustaceans, and mollusks (Pakrashi et al, 1989; Ozogul et al., 2015), given that they are produced by phytoplankton, microalgae, cyanobacteria, and terrestrial vascular plants (Volkman 1986; Saavedra et al., 2014). Sterols and hydrocarbons are recalcitrant molecules often used as tracers of biogenic material origin and transformation processes in the environment (Gagosian and Nigrelli 1979; Saavedra et al., 2014). Interestingly, we could detect their production and persistence in the SWACP sediment.

Water-sediment interface influenced by methane input

Studies report that pockmark crater shape influences local hydrodynamics (Manley et al. 2004, Hammer et al. 2009, Haverkamp et al. 2014, Schattner et al. 2016), allowing for the precipitation of nutrients on the pockmark surface leading to their concentration within the sediment profile enforced by the marine current deflection and vortex formation. This gradient of nutrients influences the microbial community within sediment depth in which bottom waters influence the inactive pockmark superficial layer (Haverkamp et al. 2014). As such, the presence of Marine Group B (MGB) of SAR324 phylum, a chemoheterotroph associated with aromatic compound degradation (Li et al., 2014) commonly detected in bottom waters, is explained and shown to be essential to pockmark microbial ecology, as it was enriched in the presence of methane. Oceanospirillales, also reported in marine bottom waters and very typical of marine sediments, are Gammaproteobacteria whose members can be sulfate reducers (Haverkamp et al. 2014), which were associated with hydrocarbon degradation in the Deepwater Horizon deep-sea hydrocarbon plume (Kleindienst et al., 2016). Surprisingly, members of the Alphaproteobacteria SAR11, commonly found in the upper pelagic system, had different ASVs present as unique in either control or enriched samples, which could have consumed methyl compounds derived from methanotrophy and methylotrophy (Sun et al., 2011), such as methanol and other short-chain alcohols. Alcohols, one of the by-products of organic matter fermentation (Dalcin Martins et al., 2019), can be further oxidized into aldehydes and fatty acids through β-oxidation, or inserted in the cell membrane (Binazadeh et al., 2009). Thus, we conclude that the water column influences SWACP deep-sea sediment microbiota, with the essential collaboration of local carbon cycling.

Entrapped methane and methanogenesis in the SWACP

A local origin of AH also includes the methane, whose probability of entrapment within the carbonate sediment was evaluated. We report environmental methane within the SWACP core sediment. This methane is a source of carbon and energy for methane-related microbial groups (Blumenberg et al. 2018), and the existence of methanotrophic taxa in our initial control sample indicates that the sediment initially supports this microbial pathway, as we had supposed. The consumption of 51% of the methane provided during the first 16h (equivalent to 10.34 $nmol.g^{-1}.h^{-1}$) was considered high compared to the methane consumption in a 10-m water layer above a pockmark in the Baltic Sea (Pimenov et al., 2008). Methane, the most abundant low-molecular-weight alkane (a short-chain acyclic saturated hydrocarbon, or aliphatic hydrocarbon), and like ethane and propane gasses, can be formed by thermal and biotic processes in deep-sea sediments (Hinrichs et al., 2006; Redmond et al., 2010; Wilkes et al., 2010; Xie et al. 2013; Blumenberg et al. 2018). However, without isotopic data from the SWACP methane, we cannot assure the origin of the entrapped methane. A biogenic origin of the methane in the SWACP could be associated with the Euryarchaeota member Methanobacteriales, which was only present in the initial control sample and vanished during incubation and methane insertion. Methanobacteriales was associated with the formation of carbonate crusts in active seeps (Heijs et al., 2006; Case et al., 2015) and with dark hydrogen oxidation and hydrogenotrophic methanogenesis (Aloisi et al., 2002). Another biogenic origin of AH relates to C11, the most abundant AH of the SWACP, which was reported to act as a pheromone in seaweed *Dictyopteris* (Zatelli et al., 2018), suggesting that benthic organisms can also provide hydrocarbons to the SWACP system.

The emission of biogenic methane is the balance of methanogenesis and methanotrophy (Hanson and Hanson, 1996). Thus, the methane detected in the headspace could have originated from the methane inserted itself, and from the one released through methanogenesis. Such methanogenesis could had been favored by the oxygen exhaustion in the airtight mini-cores, or originated from anaerobic sites within the sediment, as the entire physical-chemical and microbial stratification of the deep-sea floor was preserved in the intact core. Regarding the methane-enriched system, the community benefited from the presence of the methane itself and probably from subsequent by-products of this pathway even more after the second insertion of methane (2 times flush on the 20^{th} day). By-products of methanotrophy also compose the organic matter, and another possibility for late incubation methanogenesis could be organic matter fermentation by methyl-reducing methanogenesis (Evans et al., 2019), as methane is the terminal step of organic matter decomposition in marine sediments (Ferry et al., 2008), associated also with methylotrophic methanogenesis based on sediment DIC (Yin et al., 2019). The presence of the uncultured Methanomassiliicoccales (Thermoplasmatota), as enriched in the methane system, could be related to its potential for methylotrophy and methanogenesis by reduction of methyl-compounds using H_2 (Lang et al., 2015). In addition, the uncultured phylum RCP2-54 (formerly a deltaproteobacterial order), reported in bicarbonate-rich hot springs in China (Briggs et al., 2014) and in the methane-rich deep-sea sediment of the Barents Sea (Begmatov et al., 2021), was the keystone of the second insertion of methane (of the enriched-720h). The positive correlations in methane-rich samples between RCP2-54 with Halanaerobiaeota, Poribacteria, and Schekmanbacteria, suggest an ecological role of those rare phyla in the methane systems in the deep sea.

Fermentation, respiration/reduction, and methanogenesis (Finke and Jørgensen, 2008) are metabolisms associated with anaerobic degradation of organic matter. The positive correlation of Thermoplasmatota with Acidobacteriota and methane detection in the headspace reenforces the notion of methanogenic activity based on possibly anaerobic hydrocarbon degradation. Acidobacteria members are ubiquitous oligotrophs that are adaptable to oxygen variations (Teske and Verera, 2020) and perform diverse chemoheterotrophic metabolisms (Eichorst et al., 2018). They were recently also characterized as

polysulfide reducers (Flieder et al., 2021), the distribution of which was reported to be driven by grain size and Cu and Cr concentrations in a high hydrocarbon-contaminated marine sediment in the Mediterranean Sea (Dell'Anno et al., 2021). The same positive correlation to methane detection with Chloroflexi and Elusimicrobiota indicates that these groups could be similarly involved in anaerobic hydrocarbon degradation via fermentation (Bovio-Winkler, Cabezas and Etchebehere, 2021), giving meaning to some groups included in the "microbial dark matter" found in anaerobic sulfidic systems, such as Elusimicrobiota (Rojas et al., 2021).

Anaerobic hydrocarbon degradation influenced by methane input

Anaerobic hydrocarbon degradation is commonly found in deep and anoxic sediments, such as in asphalt and cold seeps, in sites polluted with petroleum and its by-products (Michaelis et al., 2002), as well as in situations where oxygen is consumed by aerobic hydrocarbon degradation, leading to a succession of anaerobic metabolisms (Singh et al, 2014). Strict anaerobic fermenters in Chloroflexi (Bovio-Winkler, Cabezas and Etchebehere, 2021), phylum reported within specific microbial groups of carbonate crusts (Heijs et al., 2006; Case et al., 2015) and in active seeps (Ruff et al., 2019), perpetuated along all incubation times and enrichment types, seeing as enriched in our methane-enriched system. This indicates that the local organisms play a role related to anaerobic hydrocarbon degradation in the sediment of the carbonate-enriched pockmark.

Anaerobic hydrocarbon degradation is also associated with many microbial groups that develop anaerobic respiration of nitrate, nitrite, nitrous oxide, sulfate, thiosulphate, carbonate, and metal ions, and with the groups that develop fermentation and anoxic phototrophic reactions (Michaelis et al., 2002; Grossi et al. 2008). We observed groups associated with aerobic and anaerobic pathways, the latter being detected in all samples including those enriched with methane. It is known that denitrifying bacteria can degrade different aliphatic and aromatic hydrocarbons through nitrate reduction (Grossi et al., 2008; Weelink et al., 2009). In addition, methanotrophy and methylotrophy act in communal metabolism associated with denitrification in conditions of near anaerobiosis (Kalyuzhnaya et al., 2008). In the SWACP, the biogeochemical cycle of nitrogen was sustained in the methane-enriched system, with Gammaproteobacteria members potentially involved in nitrogen respiration in addition to the nitrifiers nitrospinotal Nitrosospina (Rosenberg et al., 2014) and crenarchaeotal Nitrososphaeria (Pester et al., 2012), the latter of which is also potentially involved in CO and methane-ammonia oxidation (Lontoh et al., 2000). Interestingly, the presence of Crenarchaeota was evident only in the enriched samples from 16h to 720h, and not in the enriched-960h, suggesting the system may have become more anaerobic towards the end of incubation. However, the system was not strictly anaerobic since the aerobic alkaliphilic chemoorganotroph *Truepera,* from the Deinococcota phylum (formerly Deinoccocus-Thermus group) (Albuquerque et al., 2005) and the only recognized member of the Trueperaceae (Battista, 2016), was found only in the enriched-960h, where homolactic fermentation could also have occurred (Albuquerque et al., 2005).

Methanotrophs and non-methane hydrocarbon degradation potential influenced by methane

The basis of this discussion relies on the fact that aerobic methanotrophs enzymes MMO have a broad substrate spectrum and are capable of degrading aliphatic hydrocarbons other than methane, linear and cyclic ones from C1-C4 in the case of pMMO, and C1-C10 in the case of sMMO (Yurimoto et al., 2005, Kotani et al., 2006, Murrell and Smith, 2010, Abbasian et al., 2015). The detection of the Methylomyrabilota phylum (former candidate division NC10) as enriched taxa in the methane-enriched SWACP could be associated with its potential for methanotrophy and methylotrophy (Ettwig et al. 2008; Khadem et al., 2011; Sharp et al., 2012), and potentially even other methyl-compounds utilization.

Methanotrophs release methanol, which is consumed by methylotrophs, and facultative methylotrophs, which release formaldehyde, and

formate. These methyl-compounds are in turn consumed by non-methylotrophic heterotrophs (Yu et al., 2019). The methylotrophic oxidation product is formaldehyde, which can be converted to CO_2 by methyl-compounds oxidizers (Sun et al., 2011). Formaldehyde can be also reduced in the CO_2 fixation by autotrophic acetogenic bacteria and hydrogenotrophic methanogens, derivating into formate and CO (Lemaire, Jespersen and Wagner, 2020). Both are fixed in the central metabolism, ending up in acetate and methane as final products (Lemaire, Jespersen and Wagner, 2020). The asgardarchaeotal Lokiarchaeia is a potential reductive acetogen and aromatic hydrocarbon degrader (Farag et al., 2020). In our experiment, it was found as a methane-enriched taxon, which could be related to methylotrophic by-production in the system and to hydrocarbon degradation.

Hydrocarbon by-products of methanotrophy and methylotrophy can also be utilized by other groups of non-methylotrophic heterotrophs (Yurimoto et al., 2005; Murrell and Smith, 2010; Abbasian et al., 2015; Redmond et al., 2010; Yu et al., 2019). These groups were the methane-enriched taxa Myxococcota and Bdellovibrionota, related to predation and ectoparasites (Rosenberg et al., 2014), in addition to the gammaproteobacterial Coxiellales and verrucomicrobial Chlamidyae, related to intracellular parasitism (Hedlund, 2011). The concomitant presence of deep-sea corals on the pockmark sediment collected by chance could indicate an ecological relationship of the benthic fauna symbionts with methane cycling in the SWACP.

CONCLUSION

Using a combination of methane enrichment and 16S rRNA gene next-generation sequencing, this study characterized the methane-related microbial community of a pockmark surrounding a recently described carbonate ridge in the SW Atlantic. The SWACP represents a hotspot for chemosynthetic and chemoheterotrophic microbial groups associated with sedimented petrogenic and biogenic hydrocarbons, and local by-products originating from hydrocarbon degradation's metabolisms, non-methane, and methane, which also stimulate the non-methylotrophic heterotrophs and methanogens. Further investigations are needed to track the mineralization of the carbon from methane by the microbial community, perhaps with the use of nucleic acid-based isotope probing techniques.

ACKNOWLEDGMENTS

This research was carried out in association with the ongoing R&D project registered as ANP 21012-0, "MARINE LIFE - BMC - OIL, AND GAS SEEPS (BIOIL)" (Universidade de São Paulo / Shell Brasil / ANP) – "Biology and Geochemistry of Oil and Gas Seepages, Southwest Atlantic (BIOIL)", sponsored by Shell Brasil under the ANP R&D levy as "Compromisso de Investimentos com Pesquisa e Desenvolvimento". BIOIL Project (Shell Brasil) supported the following fellowships: AGB and FMN postdoctoral fellowships; RBR Ph.D. fellowship; ACAB Master's fellowship; and LSF Scientific Initiation fellowship. JGP was supported by Master's fellowships from the Coordenação de Aperfeiçoamento de Pessoal de Nível Superior - CAPES. MMdeM acknowledges the Conselho Nacional de Desenvolvimento Científico e Tecnológico (CNPq, grant 300962/2018-5).

We are thankful to the research teams of LECOM, Rosa C. Gamba, and Henrique dos Reis Miguel from the Oceanographic Instrumentation Laboratory (LIO/USP) for their contribution to the sampling of materials and scientific support. We thank the captain and the crew of the R/V Alpha Crucis (IO-USP, FAPESP Process number 2010/06147-5) for the essential support during the I BIOIL oceanographic cruise.

AUTHOR CONTRIBUTIONS

F.M.N.: Sampling; Investigation; Methodology; Writing – original draft; Writing – review & editing;

C.A.M.; A.C.deA.B., J.G.P.; T.H.T.: Methodology; Writing – review & editing;

A.G.B.: Sampling; Writing – review & editing;

L.F.S.; R.B.R: Sampling; Methodology; Writing – review & editing;

R.A.L.; C.N.S.: Coordination; Resources; Methodology; Writing – review & editing;

M.M.deM.: Coordination; Resources; Writing – review & editing;

P.Y.G.S.: Conceptualization; Funding Acquisition; Project Administration; Coordination; Resources; Writing – review & editing;

V.H.P.: Coordination; Supervision; Resources; Writing – review & editing.

REFERENCES

ABBASIAN, F., ROBIN, L., MEGHARAJ. M. & RAVI N. 2015. A comprehensive review of aliphatic hydrocarbon biodegradation by bacteria. *Applied Biochemistry and Biotechnology,* 176(3), 670-99.

ALBUQUERQUE, L., SIMÕES, C., NOBRE, M. F., PINO, N. M., BATTISTA, J. R., SILVA, M. T. & COSTA, M. S. 2005. Truepera Radiovictrix Gen. Nov., Sp. Nov., a new radiation resistant species and the proposal of Trueperaceae Fam. Nov. *FEMS Microbiology Letters*, 247(2), 161-169.

ALOISI, G., BOULOUBASSI, I., HEIJS, S. K., PANCOST, R. D., PIERRE, C., DAMSTÉ, J. S. S. & ROUCHY, J. M. 2002. CH_4-consuming microorganisms and the formation of carbonate crusts at cold seeps. *Earth and Planetary Science Letters,* 203(1), 195-203.

BARBERAN, A. 2016. *International Journal of Systematic and Evolutionary Microbiology (IJSEM) phenotypic database* [online]. São Paulo: Figshare. Available at: https://figshare.com/articles/dataset/International_Journal_of_Systematic_and_Evolutionary_Microbiology_IJSEM_phenotypic_database/4272392/3. [Accessed: 2020, July. 11].

BARTRAM, A. K., CALVIN, P. & NEUFELD, J. D. 2009. Nucleic acid contamination of glycogen used in nucleic acid precipitation and assessment of linear polyacryl amide as an alternative co-precipitant. *Biotechniques*, 47(6), 1019-1022.

BASTIAN, M., HEYMANN, S. & JACOMY, M. 2009. Gephi: an open source software for exploring and manipulating networks. *Proceedings of the International AAAI Conference on Web and Social Media*, 3(1), 361-362.

BATTISTA, J. R. 2016. *Deinococcus-thermus group*. Rio de Janeiro: eLS, pp. 1-12.

BEGMATOV, S., SAVVICHEV, A. S., KADNIKOV, V. V., BELETSKY, A. V., RUSANOV, I. I., KLYUVITKIN, A. A. & RAVIN, N. V. 2021. Microbial communities involved in methane, sulfur, and nitrogen cycling in the sediments of the Barents sea. *Microorganisms*, 9(11), 2362.

BENDIA, A. G., SIGNORI, C. N., NAKAMURA, F. M., BUTARELLI, A. C. D. A., PASSOS, J. G., RAMOS, R. B. & PELLIZARI, V. H. 2021. Microbial perspective on the giant carbonate ridge Alpha Crucis (Southwestern Atlantic upper slope). *FEMS Microbiology Ecology*, 97(8), fiab110.

BINAZADEH, M., KARIMI, I. A. & LI, Z. 2009. Fast biodegradation of long chain n-alkanes and crude oil at high concentrations with Rhodococcus sp. Moj-3449. *Enzyme and Microbial Technology*, 45(3), 195-202.

BLUMENBERG, M., PAPE, T., SEIFERT, R., BOHRMANN, G. & SCHLÖMER, S. 2018. Can hydrocarbons entrapped in seep carbonates serve as gas geochemistry recorder?. *Geo-Marine Letters*, 38(2), 121-129.

BOLYEN, E., RIDEOUT, J. R., DILLON, M. R., BOKULICH, N. A., ABNET, C. C., AL-GHALITH, G. A., BISANZ, J. E., BITTINGER, K., BREJNROD, A., BRISLAWN, C. J., BROWN, C. T., CALLAHAN, B. J., CARABALLO-RODRÍGUEZ, A. M., CHASE, J., COPE, E. K., SILVA, R., DIENER, C., DORRESTEIN, P. C., DOUGLAS, G. M., DURALL, D. M., DUVALLET, C., EDWARDSON, C. F., ERNST, M., ESTAKI, M., FOUQUIER, J., GAUGLITZ, J. M., GIBBONS, S. M., GIBSON, D. L., GONZALEZ, A., GORLICK, K., GUO, J., HILLMANN, B., HOLMES, S., HOLSTE, H., HUTTENHOWER, C., HUTTLEY, G. A., JANSSEN, S., JARMUSCH, A. K., JIANG, L., KAEHLER, B. D., KANG, K. B., KEEFE, C. R., KEIM, P., KELLEY, S. T., KNIGHTS, D., KOESTER, I., KOSCIOLEK, T., KREPS, J., LANGILLE, M. G. I., LEE, J., LEY, R., LIU, Y. X., LOFTFIELD, E., LOZUPONE, C., MAHER, M., MAROTZ, C., MARTIN, B. D., MACDONALD, D., ZECH XU, Z., ZANEVELD, J. R., ZHANG, Y., ZHU, Q., KNIGHT R. & CAPORASO, J. G. 2019. Reproducible, interactive, scalable and extensible microbiome data science using QIIME 2. *Nature Biotechnology*, 37(8), 852-857.

BOVIO-WINKLER, P., CABEZAS, A. & ETCHEBEHERE, C. 2021. Database mining to unravel the ecology of the phylum chloroflexi in methanogenic full-scale bioreactors. *Frontiers in Microbiology,* 11, 3608.

BRIGGS, B. R., BRODIE, E. L., TOM, L. M., DONG, H., JIANG, H., HUANG, Q. & HUNGATE, B. A. 2014. Seasonal patterns in microbial communities inhabiting the hot springs of Tengchong, Yunnan Province, China. *Environmental Microbiology*, 16(6), 1579-1591.

BUNYOLA, P. F., MARANTE, F. J. T., OYOLA, J. F. L., MARTIN, I. B., ALONSO, R. G. & RODRÍGUEZ, J. J. S. 2018. Chemical constituents derived from the Canaries marine sponge *Myxilla* sp. *Química Nova*, 41(3), 292-296.

CALLAHAN, B. J., MCMURDIE, P. J. & HOLMES, S. P. 2017. Exact sequence variants should replace operational taxonomic units in marker-gene data analysis. *The ISME Journal*, 11(12), 2639-2643.

CASE, D. H., PASULKA, A. L., MARLOW, J. J., GRUPE, B. M., LEVIN, L. A. & ORPHAN, V. J. 2015. Methane seep carbonates host distinct, diverse, and dynamic microbial assemblages. *mBio*, 6(6), e01348-15.

COMANDINI, A., DUBOIS, T., ABID, S. & CHAUMEIX, N. 2013. Comparative study on cyclohexane and decalin oxidation. *Energy & Fuels*, 28(1), 714-724.

CONWAY, N. M. 1994. Stable isotope in the study of marine chemosynthetic-based ecosystems. *Stable Isotopes in Ecology,* 158-186.

CONWAY, J. R., LEX, A. & GEHLENBORG, N. 2017. UpSetR: an R package for the visualization of intersecting sets and their properties. *Bioinformatics*, 33(18), 2938-2940

DANDO, P. R., AUSTEN, M. C., BURKE JUNIOR, R. A., KENDALL, M. A., KENNICUTT, M. C., JUDD, A. G. & SOUTHWARD, A. J. 1991. Ecology of a North Sea pockmark with an active methane seep. *Marine Ecology Progress Series*, 70, 49-63.

DE MAHIQUES, M. M., SCHATTNER, U., LAZAR, M., SUMIDA, P. Y. G. & DE SOUZA, L. A. P. 2017. An extensive pockmark field on the upper Atlantic margin of Southeast Brazil: spatial analysis and its relationship with salt diapirism. *Heliyon*, 3(2), e00257.

DELL'ANNO, F., RASTELLI, E., TANGHERLINI, M., CORINALDESI, C., SANSONE, C., BRUNET, C., BALZANO, S., IANORA, A., MUSCO, L., MONTEREALI, M. R. & DELL'ANNO, A. 2021. Highly contaminated marine sediments can host rare bacterial taxa potentially useful for bioremediation. *Frontiers in Microbiology*, 12, 326.

EICHORST, S. A., TROJAN, D., ROUX, S., HERBOLD, C., RATTEI, T. & WOEBKEN, D. 2018. Genomic insights into the Acidobacteria reveal strategies for their success in terrestrial environments. *Environmental Microbiology*, 20(3), 1041-1063.

ETTWIG, K. F., SHIMA, S., VAN DE PAS-SCHOONEN, K. T., KAHNT, J., MEDEMA, M. H., OP DEN CAMP, H. J. & STROUS, M. 2008. Denitrifying bacteria anaerobically oxidize methane in the absence of Archaea. *Environmental Microbiology*, 10(11), 3164-3173.

EVANS, P. N., BOYD, J. A., LEU, A. O., WOODCROFT, B. J., PARKS, D. H., HUGENHOLTZ, P. & TYSON, G. W. 2019. An evolving view of methane metabolism in the Archaea. *Nature Reviews Microbiology*, 17(4), 219-232.

FARAG, I. F., BIDDLE, J. F., ZHAO, R., MARTINO, A. J., HOUSE, C. H. & LEÓN-ZAYAS, R. I. 2020. Metabolic potentials of archaeal lineages resolved from metagenomes of deep Costa Rica sediments. *The ISME Journal*, 14(6), 1345-1358.

FELDEN, J., WENZHÖFER, F., FESEKER, T. & BOETIUS, A. 2010. Transport and consumption of oxygen and methane in different habitats of the Håkon Mosby Mud Volcano (HMMV). *Limnology and Oceanography*, 55(6), 2366-2380.

FERRY, J. G. & LESSNER, D. J. 2008. Methanogenesis in marine sediments. *Annals of the New York Academy of Sciences*, 1125(1), 147-157.

FIGUEIREDO JUNIOR, A. G., BREHME, I., BARBOSA, K. F., NETO, J. A. B. & SILVA, C. G. 1999. Sea-floor depressions in Paraná continental shelf, Santos Basin. *In: 6th International Congress of the Brazilian Geophysical Society* (pp. cp-215). European Association of Geoscientists & Engineers.

FINKE, N. & JØRGENSEN, B. B. 2008. Response of fermentation and sulfate reduction to experimental temperature changes in temperate and Arctic marine sediments. *The ISME Journal*, 2(8), 815-829.

FLIEDER, M., BUONGIORNO, J., HERBOLD, C. W., HAUSMANN, B., RATTEI, T., LLOYD, K. G. & WASMUND, K. 2021. Novel taxa of Acidobacteriota implicated in seafloor sulfur cycling. *The ISME journal*, 15(11), 3159-3180.

GAGOSIAN, R. B. & NIGRELLI, G. E. 1979. The transport and budget of sterols in the western North Atlantic Ocean 1, 2. *Limnology and oceanography*, 24(5), 838-849.

GROSSI, V., CRAVO-LAUREAU, C., GUYONEAUD, R., RANCHOU-PEYRUSE, A. & HIRSCHLER-RÉA, A. 2008. Metabolism of n-alkanes and n-alkenes by anaerobic bacteria: a summary. *Organic Geochemistry,* 39(8), 1197-1203.

HAFIDZ, Y., ZAINI, A. & SAMSUR, M. 2012. Aliphatic hydrocarbons in surface sediments from South China Sea off Kuching Division, Sarawak. *Malaysian Journal of Analytical Sciences*, 16(1), 1-11.

HAMMER, Ø., WEBB, K. E. & DEPREITER, D. 2009. Numerical simulation of upwelling currents in pockmarks, and data from the Inner Oslofjord, Norway. *Geo-Marine Letters*, 29(4), 269-275.

HANSON, R. S. & HANSON, T. E. 1996. Methanotrophic bacteria. *Microbiological Reviews*, 60(2), 439-471.

HARRELL JUNIOR, F. E. & HARRELL JUNIOR, M. F. E. 2019. *Package 'hmisc'*. Vienna: The R Foundation, pp. 235-236.

HAVERKAMP, T. H., HAMMER, Ø. & JAKOBSEN, K. S. 2014. Linking geology and microbiology: inactive pockmarks affect sediment microbial community structure. *PloS One*, 9(1), e85990.

HEDLUND, B. P. 2010. Phylum XXIII. Verrucomicrobia phyl. nov. *In:* KRIEG, N. R., STALEY, J. T., BROWN, D. R., HEDLUND, B. P., PASTER, B. J., WARD, N. L., LUDWIG, W. & WHITMAN, W. B. (eds.). *Bergey's manual® of systematic bacteriology*. New York: Springer, pp. 795-841.

HEIJS, S. K., ALOISI, G., BOULOUBASSI, I., PANCOST, R. D., PIERRE, C., DAMSTÉ, J. S. S. & FORNEY, L. J. 2006. Microbial community structure in three deep-sea carbonate crusts. *Microbial Ecology*, 52(3), 451-462.

HINRICHS, K. U., HAYES, J. M., BACH, W., SPIVACK, A. J., HMELO, L. R., HOLM, N. G. & SYLVA, S. P. 2006. Biological formation of ethane and propane in the deep marine subsurface. *Proceedings of the National Academy of Sciences*, 103(40), 14684-14689.

JENG, W. L. & HUH, C. A. 2004. Lipids in suspended matter and sediments from the East China Sea Shelf. *Organic Geochemistry*, 35(5), 647-660.

JOYE, S. B., BOETIUS, A., ORCUTT, B. N., MONTOYA, J. P., SCHULZ, H. N., ERICKSON, M. J. & LUGO, S. K. 2004. The anaerobic oxidation of methane and sulfate reduction in sediments from Gulf of Mexico cold seeps. *Chemical Geology*, 205(3-4), 219-238.

KALYUZHNAYA, M. G., LAPIDUS, A., IVANOVA, N., COPELAND, A. C., MCHARDY, A. C., SZETO, E., SALAMOV, A., GRIGORIEV, I. V., SICIU, D., LEVINE, S. R., MARKOWITZ, V. M., RIGOUTSOS, I., TRINGE, S. G., BRUCE, D. C., RICHARDSON, P. M., LIDSTROM, M. E. & CHISTOSERDOVA, L. 2008. High-resolution metagenomics targets specific functional types in complex microbial communities. *Nature Biotechnology*, 26(9), 1029-1034.

KATOH, K., ASIMENOS, G. & TOH, H. 2009. Multiple alignment of DNA sequences with MAFFT. *Methods in Molecular Biology*, 2009;537:39-64.

KAWAMURA, K. 1995. Land-derived lipid class compounds in the deep-sea sediments and marine aerosols from North Pacific. *Biogeochemical Processes and Ocean Flux in the Western Pacific*, 1, 31-51.

KHADEM, A. F., POL, A., WIECZOREK, A., MOHAMMADI, S. S., FRANCOIJS, K. J., STUNNENBERG, H. G., JETTEN, M. S. M. & OP DEN CAMP, H. J. 2011. Autotrophic methanotrophy in Verrucomicrobia: Methylacidiphilum fumariolicum SolV uses the Calvin-Benson-Bassham cycle for carbon dioxide fixation. *Journal of bacteriology*, 193(17), 4438-4446.

KLEINDIENST, S., GRIM, S., SOGIN, M., BRACCO, A., CRESPO-MEDINA, M. & JOYE, S. B. 2016. Diverse, rare microbial taxa responded to the Deepwater Horizon deep-sea hydrocarbon plume. *The ISME Journal*, 10(2), 400-415.

KOTANI, T., KAWASHIMA, Y., YURIMOTO, H., KATO, N. & SAKAI, Y. 2006. Gene structure and regulation of alkane monooxygenases in propane-utilizing Mycobacterium sp. TY-6 and Pseudonocardia sp. TY-7. *Journal of Bioscience and Bioengineering*, 102(3), 184-192.

LANG, K., SCHULDES, J., KLINGL, A., POEHLEIN, A., DANIEL, R. & BRUNE, A. 2015. New mode of energy metabolism in the seventh order of methanogens as revealed by comparative genome analysis of "Candidatus Methanoplasma termitum". *Applied and Environmental Microbiology*, 81(4), 1338-1352.

LEMAIRE, O. N., JESPERSEN, M. & WAGNER, T. 2020. CO_2-fixation strategies in energy extremophiles: what can we learn from acetogens?. *Frontiers in Microbiology*, 11, 486.

LI, M., JAIN, S., BAKER, B. J., TAYLOR, C. & DICK, G. J. 2014. Novel hydrocarbon monooxygenase genes in the metatranscriptome of a natural deep-sea hydrocarbon plume. *Environmental Microbiology*, 16(1), 60-71.

LONTOH, S., DISPIRITO, A. A., KREMA, C. L., WHITTAKER, M. R., HOOPER, A. B. & SEMRAU, J. D. 2000. Differential inhibition *in vivo* of ammonia monooxygenase, soluble methane monooxygenase and membrane-associated methane monooxygenase by phenylacetylene. *Environmental Microbiology*, 2(5), 485-494.

LOUCA, S., PARFREY, L. W. & DOEBELI, M. 2016. Decoupling function and taxonomy in the global ocean microbiome. *Science*, 353(6305), 1272-1277.

LOURENÇO, R. A., BLANCO, J., SILVA, J. & TANIGUCHI, S. 2021. Can the environmental health of urban centers be assessed through pollutants trapped in lakes? A study case in the biggest city of the southern hemisphere. *Environmental Science and Pollution Research*, 28(24), 30774-30782.

LOZUPONE, C., LLADSER, M. E., KNIGHTS, D., STOMBAUGH, J. & KNIGHT, R. 2011. UniFrac: an effective distance metric for microbial community comparison. *The ISME Journal*, 5(2), 169-172.

MALY, M., SCHATTNER, U., LOBO, F. J., DIAS, R. J. S., RAMOS, R. B., COUTO, D. D. M. & MAHIQUES, M. M. 2019. The Alpha Crucis Carbonate Ridge (ACCR): discovery of a giant ring-shaped carbonate complex on the SW Atlantic margin. *Scientific Reports*, 9(1), 1-10.

MANDAL, S., VAN TREUREN, W., WHITE, R. A., EGGESBØ, M., KNIGHT, R. & PEDDADA, S. D. 2015. Analysis of composition of microbiomes: a novel method for studying microbial composition. *Microbial Ecology in Health and Disease*, 26(1), 27663.

MANLEY, P. L., MANLEY, T. O., WATZIN, M. C. & GUTIERREZ, J. 2004. Lakebed pockmarks in Burlington Bay, Lake Champlain: I. Hydrodynamics and implications of origin. *In:* MANLEY, P. L., MANLEY, T. O. & MIHUC, T. B. (eds.). *Lake Champlain: partnerships and research in the new millennium*. Boston: Springer, pp. 299-329.

MANN, S. & CHEN, Y. P. P. 2010. Bacterial genomic G+C composition-eliciting environmental adaptation. *Genomics*, 95(1), 7-15.

MARCON, Y., ONDREAS, H., SAYUSOFFHLING, H., BOHRMANN, G. & OLU, K. 2013. Fluid flow regimes and growth of a giant pockmark. *Geology*, 42(1), 63-66.

MARTINS, P. D., FRANK, J., MITCHELL, H., MARKILLIE, L. M. & WILKINS, M. J. 2019. Wetland sediments host diverse microbial taxa capable of cycling alcohols. *Applied and Environmental Microbiology*, 85(12), e00189-19.

MCGENITY, T. J., MCKEW, B. A. & LEA-SMITH, D. J. 2021. Cryptic microbial hydrocarbon cycling. *Nature Microbiology*, 6(4), 419-420.

MCMURDIE, P. J. & HOLMES, S. 2013. Phyloseq: an R package for reproducible interactive analysis and graphics of microbiome census data. *PLoS One*, 8(4), e61217.

MICHAELIS, W., SEIFERT, R., NAUHAUS, K., TREUDE, T., THIEL, V., BLUMENBERG, M., KNITTEL, K., GIESEKE, A., PETERKNECHT, K., PAPE, T., BOETIUS, A., AMANN, R., JØRGENSEN, B. B., WIDDEL, F., PECKMANN, J., PIMENOV, N. V. & GULIN, M. B. 2002. Microbial reefs in the Black Sea fueled by anaerobic oxidation of methane. *Science*, 297(5583), 1013-1015.

MILLE, G., ASIA, L., GUILIANO, M., MALLERET, L. & DOUMENQ, P. 2007. Hydrocarbons in coastal sediments from the Mediterranean Sea (Gulf of Fos area, France). *Marine Pollution Bulletin*, 54(5), 566-575.

MUDGE, S. M. 2005. Fatty alcohols—a review of their natural synthesis and environmental distribution. *The Soap and Detergent Association,* 132, 1-141.

MURRELL, J. C. & SMITH, T. J. 2010. Biochemistry and molecular biology of methane monooxygenase. *In:* TIMMIS, K. N. (ed.). *Handbook of hydrocarbon and lipid microbiology.* New York: Springer, pp. 1045-1055.

NAGEL, F. 2020. *Linking methane fluxes and oxidation rates to methane oxidizing bacteria in an Arctic terrestrial methane seep, Svalbard*. MSc. Norges: UiT Norges Arktiske Universitet.

NAKAYAMA, C. R., KUHN, E., ARAÚJO, A. C. V., ALVALÁ, P. C., FERREIRA, W. J., VAZOLLER, R. F. & PELLIZARI, V. H. 2011. Revealing archaeal diversity patterns and methane fluxes in Admiralty Bay, King George Island, and their association to Brazilian Antarctic Station activities. *Deep Sea Research Part II: Topical Studies in Oceanography*, 58(1-2), 128-138.

OKSANEN, J., BLANCHET, F. G., KINDT, R., LEGENDRE, P., MINCHIN, P. R., O'HARA, R. B. & OKSANEN, M. J. 2013. Package 'vegan'. *Community ecology package*, 2(9), 1-295.

OZOGUL, F., KULEY, E. & OZOGUL, Y. 2015. Sterol content of fish, crustacea and mollusc: effects of cooking methods. *International Journal of Food Properties*, 18(9), 2026-2041.

PAKRASHI, S. C., DUUTTA, P. K., ACHARI, B., MISRA, S., CHOUNDHURY, A., CHATTOPADHYAY, S. & GHOST, A. 1989. Lipids and fatty acids of the horseshoe crabs Tachypleus gigas and Carcinoscorpius rotundicauda. *Lipids*, 24(5), 443-447.

PARADA, A. E., NEEDHAM, D. M. & FUHRMAN, J. A. 2016. Every base matters: assessing small subunit rRNA primers for marine microbiomes with mock communities, time series and global field samples. *Environmental microbiology*, 18(5), 1403-1414.

PARTE, A. C. 2018. LPSN-List of Prokaryotic names with Standing in Nomenclature (bacterio. net), 20 years on. *International Journal of Systematic and Evolutionary Microbiology*, 68(6), 1825-1829.

PAULL, C., USSLER III, W., MAHER, N., GREENE, H. G., REHDER, G., LORENSON, T. & LEE, H. 2002. Pockmarks off Big Sur, California. *Marine Geology*, 181(4), 323-335.

PESTER, M., RATTEI, T., FLECHL, S., GRÖNGRÖFT, A., RICHTER, A., OVERMANN, J. & WAGNER, M. 2012. amoA-based consensus phylogeny of ammonia-oxidizing archaea and deep sequencing of amoA genes from soils of four different geographic regions. *Environmental Microbiology*, 14(2), 525-539.

PIMENOV, N. V., UL'YANOVA, M. O., KANAPATSKII, T. A., SIVKOV, V. V. & IVANOV, M. V. 2008. Microbiological and biogeochemical processes in a pockmark of the Gdansk Depression, Baltic Sea. *Microbiology*, 77(5), 579-586.

PRICE, M. N., DEHAL, P. S. & ARKIN, A. P. 2009. FastTree: computing large minimum evolution trees with profiles instead of a distance matrix. *Molecular Biology and Evolution*, 26(7), 1641-1650.

PUSCEDDU, A., DELL'ANNO, A., FABIANO, M. & DANOVARO, R. 2009. Quantity and bioavailability of sediment organic matter as signatures of benthic trophic status. *Marine Ecology Progress Series*, 375, 41-52.

REDMOND, M. C., VALENTINE, D. L. & SESSIONS, A. L. 2010. Identification of novel methane-, ethane-, and propane-oxidizing bacteria at marine hydrocarbon seeps by stable isotope probing. *Applied and Environmental Microbiology,* 76(19), 6412-22.

ROJAS, C. A., TORIO, A. S., PARK, S., BOSAK, T. & KLEPAC-CERAJ, V. 2021. Organic electron donors and terminal electron acceptors structure anaerobic microbial communities and interactions in a permanently stratified sulfidic lake. *Frontiers in microbiology*, 12, 847.

ROSENBERG, E., DELONG, E. F., LORY, S., STACKEBRANDT, E. & THOMPSON, F. 2014. *The prokaryotes: deltaproteobacteria and epsilonproteobacteria*. Berlin: Springer.

RUFF, S. E., FELDEN, J., GRUBER-VODICKA, H. R., MARCON, Y., KNITTEL, K., RAMETTE, A. & BOETIUS, A. 2019. In situ development of a methanotrophic microbiome in deep-sea sediments. *The ISME journal,* 13(1), 197-213.

SAAVEDRA, L., QUINONES, R. A., & BECERRA, J. 2014. Distribution and sources of phytosterols in coastal and river sediments of South Central Chile. *Latin American Journal of Aquatic Research*, 42(1), 61-84.

SCHATTNER, U., LAZAR, M., SOUZA, L. A. P., TEN BRINK, U. & MAHIQUES, M. M. D. 2016. Pockmark asymmetry and seafloor currents in the Santos Basin offshore Brazil. *Geo-Marine Letters*, 36(6), 457-464.

SHARP, C., STOTT, M. & DUNFIELD, P. 2012. Detection of autotrophic verrucomicrobial methanotrophs in a geothermal environment using stable isotope probing. *Frontiers in Microbiology*, 3, 303.

SIBUET, M. & OLU, K. 1998. Biogeography, biodiversity and fluid dependence of deep-sea cold-seep communities at active and passive margins. *Deep Sea Research Part II: Topical Studies in Oceanography*, 45(1-3), 517-567.

SINGH, A., HAMME, J. D. V., KUHAD, R. C., PARMAR, N. & WARD, O. P. 2014. Subsurface petroleum microbiology. *In:* PARMAR, N. & SINGH, A. (eds.). *Geomicrobiology and biogeochemistry*. Heidelberg: Springer, pp. 153-173.

STEEMANN-NIELSEN, E. 1952. The use of radio-active carbon (C^{14}) for measuring organic production in the sea. *ICES Journal of Marine Science*, 18(2), 117-140.

SUMIDA, P. Y. G., PELLIZARI, V. H., LOURENÇO, R. A., SIGNORI, C. N., BENDIA, A. G., CARRERETTE, O. & MAHIQUES, M. M. D. 2022. Seep hunting in the Santos Basin, Southwest Atlantic: sampling strategy and employed methods of the multidisciplinary cruise BIOIL 1. *Ocean and Coastal Research*, 70(Suppl 2), e22031.

SUMIDA, P. Y. G., YOSHINAGA, M. Y., MADUREIRA, L. A. S. P. & HOVLAND, M. 2004. Seabed pockmarks associated with deepwater corals off SE Brazilian Continental Slope, Santos Basin. *Marine Geology*, 207(1-4), 159-167.

SUN, J., STEINDLER, L., THRASH, J. C., HALSEY, K. H., SMITH, D. P., CARTER, A. E., LANDRY, Z. C. & GIOVANNONI, S. J. 2011. One carbon metabolism in SAR11 pelagic marine bacteria. *PloS One*, 6(8), e23973.

TEIXEIRA, C. 1973. Introdução aos métodos para medir a produção primária do fitoplâncton marinho. *Boletim do Instituto Oceanográfico*, 22, 59-92.

TESKE, A. & CARVALHO, V. 2020. *Marine hydrocarbon seeps: microbiology and biogeochemistry of a global marine habitat*. New York: Springer Nature.

TREVIZANI, T. H., NAGAI, R. H., FIGUEIRA, R. C. L., SUMIDA, P. Y. G. & MAHIQUES, M. M. D. 2022. Chemical characterization of deep-sea corals from the continental slope of Santos Basin (southeastern Brazilian upper margin). *Ocean and Coastal Research*, 70(Suppl 2), e22018.

VOLKMAN, J. K. 1986. A review of sterol markers for marine and terrigenous organic matter. *Organic Geochemistry*, 9(2), 83-99.

WANG, Z. & FINGAS, M. F. 2003. Development of oil hydrocarbon fingerprinting and identification techniques. *Marine Pollution Bulletin*, 47(9-12), 423-452.

WANG, Z., FINGAS, M. & PAGE, D. S. 1999. Oil spill identification. *Journal of Chromatography A*, 843(1-2), 369-411.

WEELINK, S. A. B., SMIDT, H., SAIA, F., RIJPSTRA, I., RÖLING, W., STAMS, A. J. M. & VAN DOESBURG, W. C. J. 2009. A strictly anaerobic betaproteobacterium Georgfuchsia toluolica gen. nov., sp. nov. degrades aromatic compounds with Fe(III), Mn(IV) or nitrate as an electron acceptor. *FEMS Microbiology Ecology,* 70(3), 575.

WICKHAM, H., CHANG, W., HENRY, L., TAKAHASHI, K., WILKE, C., WOO, K., YUTANI, H. & DUNNINGTON, D. 2016. Package 'ggplot2'. Create elegant data visualisations using the grammar of graphics. *Version*, 2(1), 1-189.

WILKES, H., JARLING, R. & SCHWARZBAUER, J. 2020. Hydrocarbons and lipids: an introduction to structure, physicochemical properties, and natural occurrence. *In:* WILKES, H. (ed.). *Hydrocarbons, Oils and Lipids: Diversity, Origin, Chemistry and Fate.* New York: Springer, pp. 3-48.

XIE, S., LAZAR, C. S., LIN, Y. S., TESKE, A. & HINRICHS, K. U. 2013. Ethane- and propane-producing potential and molecular characterization of an ethanogenic enrichment in an anoxic estuarine sediment. *Organic Geochemistry*, 59, 37-48.

YILMAZ, P., PARFREY, L. W., YARZA, P., GERKEN, J., PRUESSE, E., QUAST, C. & GLÖCKNER, F. O. 2014. The SILVA and "all-species living tree project (LTP)" taxonomic frameworks. *Nucleic Acids Research*, 42(D1), D643-D648.

YIN, X., WU, W., MAEKE, M., RICHTER-HEITMANN, T., KULKARNI, A. C., ONI, O. E. & FRIEDRICH, M. W. 2019. CO_2 conversion to methane and biomass in obligate methylotrophic methanogens in marine sediments. *The ISME Journal,* 13(8), 2107-2119.

YU, Z., ZHENG, Y., HUANG, J. & CHISTOSERDOVA, L. 2019. Systems biology meets enzymology: recent insights into communal metabolism of methane and the role of lanthanides. *Current Issues in Molecular Biology*, 33(1), 183-196.

YUNKER, M. B., MACDONALD, R. W., VINGARZAN, R., MITCHELL, R. H., GOYETTE, D. & SYLVESTRE, S. 2002. PAHs in the Fraser River basin: a critical appraisal of PAH ratios as indicators of PAH source and composition. *Organic Geochemistry,* 33(4), 489-515.

YURIMOTO, H., KATO, N. & SAKAI, Y. 2005. Assimilation, dissimilation, and detoxification of formaldehyde, a central metabolic intermediate of methylotrophic metabolism. *The Chemical Record,* 5(6), 367-375.

ZATELLI, G. A., PHILIPPUS, A. C. & FALKENBERG, M. 2018. An overview of odoriferous marine seaweeds of the Dictyopteris Genus: insights into their chemical diversity, biological potential and ecological roles. *Revista Brasileira de Farmacognosia*, 28(2), 243-260.

ZENG, E. Y., KHAN, A. R. & TRAN, K. 1997. Organic pollutants in the coastal marine environment off San Diego, California. 3. Using linear alkylbenzenes to trace sewage-derived organic materials. *Environmental Toxicology and Chemistry: An International Journal*, 16(2), 196-201.

ZRAFI, I., HIZEM, L., CHALGHMI, H., GHRABI, A., ROUABHIA, M. & SAIDANE-MOSBAHI, D. 2013. Aliphatic and aromatic biomarkers for petroleum hydrocarbon investigation in marine sediment. *Journal of Petroleum Science Research (JPSR),* 2(4), 145.